Magnetic and electric dipole transitions in MgO:V^{2+}. Shape of the zero-phonon lines

G. Viliani, O. Pilla, and M. Montagna
Dipartimento di Fisica, Università di Trento, 38050 Povo, Trento, Italy, and Gruppo Nazionale di Struttura della Materia del Consiglio Nazionale delle Ricerche, Trento, Italy

A. Boyrivent
Groupe de Spectroscopie des Solides (E.R. 10), Université Claude Bernard, Campus de La Doua, 69622 Villeurbanne, France

(Received 29 April 1980)

Excitation spectra of divalent vanadium in MgO are reported. An accurate analysis of previously unobserved transitions is presented; the magnetic and vibration-induced electric dipole contributions are discussed; and experimental energies and intensities are compared to computed ones. The role of spin-orbit interaction, Jahn-Teller effect, and nonradiative transitions in determining the shape of the zero-phonon lines are discussed.

I. INTRODUCTION

Transition-metal ions contained as substitutional impurities in cubic crystals have been the object of many studies. The interest of such studies stems from the wide variety of information one can gain on the electronic states, the electron-phonon interaction, and related phenomena (Jahn-Teller and Ham effects, and so on); in fact, the optical spectra of, for instance, d^3 ions (V^{2+}, Cr^{3+}, Mn^{4+}) show sharp zero-phonon lines (ZPL) and broad multiphonon sidebands. In particular, in the present paper we shall study the optical characteristics of MgO:V^{2+}. Since in this crystal the environment of V^{2+} has cubic symmetry[1] the states have definite parity; the lowest states originating from the d^3 configuration are even. Consequently the electric dipole (ED) transitions among them are forbidden, but are magnetic dipole (MD) or electric quadrupole allowed. Moreover, transitions between the $^4A_{2g}$ ground state and the doublet states (^2E_g, $^2T_{1g}$, $^2T_{2g}$) are also spin forbidden, and become slightly allowed by spin-orbit mixing with the quadruplet states and in particular with $^4T_{2g}$. However, odd vibrations can couple the d^3 states with higher states deriving from odd electronic configurations (d^2p, charge transfer, etc.); in this way ED transitions are observed which involve creation or annihilation of one odd phonon.

For instance, magnetic circular dichroism (MCD) and stress measurements of Sugano *et al.*[2] on MgO:Cr^{3+} and of Sturge[3,4] on MgO:V^{2+} showed the $^2E_g \rightarrow {}^4A_{2g}$ ZPL transition to be of MD character; on the contrary the sideband of such emission has been found to be ED.[5–7] This is a very favorable situation for studying the MD and ED contributions separately, because they are well separated in energy. In fact, the $^4A_{2g}$ and ^2E_g states (deriving from the strong crystal-field t_{2g}^3 configuration) are very weakly coupled to the phonons of any symmetry so that the MD intensity is practically all concentrated in the ZPL transition.

On the other hand, the $^4T_{2g}$ state is rather strongly coupled to the vibrations and its sideband has both ED and MD characters, while the ZPL is only MD.[4] The $^4A_{2g} \rightarrow {}^4T_{1g}$ transition, consisting of a broad unstructured band, is thought of as being mostly ED induced by odd phonons, since the MD transition probability vanishes by symmetry.

In the present paper, besides the transitions to the above-mentioned states, we will also show the $^4A_{2g} \rightarrow {}^2E_g$ absorption sideband, which so far has been studied only in emission, as well as the weak features corresponding to the $^4A_{2g} \rightarrow {}^2T_{1g}$ and $^4A_{2g} \rightarrow {}^2T_{2g}$ transitions. The observation of these features is possible in MgO:V^{2+}, contrary to, for instance, MgO:Cr^{3+} (Refs. 8 and 9) because luckily enough in this system the very weak $^4A_{2g} \rightarrow {}^2T_{2g}$ transition falls just in the energy range between the $^4T_{2g}$ and $^4T_{1g}$ strong bands; moreover the energy of $^2T_{1g}$ is low enough with respect to $^4T_{2g}$ as to allow the sidebands not to be masked by this latter band.

In Sec. II we describe the experimental apparatus and present the results; in Sec. III the experimental results relative to MD transitions are discussed and compared to computed energies and intensities; Sec. IV is devoted to ED transitions; in Sec. V the

electron-phonon interaction within the $^4T_{2g}$ level is considered both as regards the relative intensities of the ZPL's components and, more generally, as regards the shape of the various ZPL's.

II. EXPERIMENTAL

The MgO:V^{2+} sample, provided by the Norton Company (Canada) and containing nominally 500 ppm vanadium, was reduced at 1200 °C for 12 h in hydrogen flux. Such treatment increased the V^{2+} concentration by about a factor of 100, even though the optical quality of the crystal was somewhat worsened. However, it is important to note, for our purposes, that the residual V^{3+} still gives rise to strong and broad absorption bands through the whole spectral region of V^{2+} absorption, so that the absorption spectrum of V^{2+} alone can be observed only through the excitation spectrum of its characteristic and intense 11500-cm^{-1} emission line (R line), corresponding to the $^2E_g \rightarrow {}^4A_{2g}$ transition.[3] In this regard, it should be noted that the excitation spectrum differs from the absorption spectrum for at least two reasons: (a) different absorption by V^{3+} in different spectral regions; and (b) nonradiative transitions from the excited states to the ground state, which cause different amounts of excitation to be fed into the ^2E_g state from the different excited levels.

The mechanism of nonradiative decay is, in general, not well known, and especially so for such a complicated multilevel system like V^{2+}, where many spin-orbit levels are interacting nonradiatively and where orbital degeneracy introduces a further complication through the Jahn-Teller effect. We can get a qualitative idea of what is going on by the existing results on the isoelectronic ion Cr^{3+} where the quantum yield of the $^2E_g \rightarrow {}^4A_{2g}$ transition is found to be ~ 0.4.[10,11] In the same system, the intensity ratio

$$I(^4A_{2g} \rightarrow {}^4T_{2g})/I(^4A_{2g} \rightarrow {}^4T_{1g})$$

calculated by the excitation spectrum of the R line is found to be 3–4 times as intense as the ratio deduced from absorption spectra,[8] indicating that these two excited states have different decay mechanisms possibly due to energy transfer to different centers.

On the other hand, since the nonradiative $^4T_{2g} \rightarrow (^2T_{1g}, {}^2E_g)$ transitions are extremely fast ($\sim 10^{-13}$ sec, see Sec. V) it is to be expected that other deexcitation channels do not contribute appreciably, so that the excitation spectrum should reproduce the absorption one quite faithfully. Moreover, the total luminescence intensity was found to be temperature independent,[5] which shows that the nonradiative transitions to the ground state (which are expected to be strongly temperature dependent) are not very important.

In spite of the difficulties connected with the excitation spectrum, this latter has important advantages with respect to the absorption spectrum. In fact, it allows much weaker features (about three orders of magnitude with respect to the more intense bands) to be measured, which would probably be masked by competitive absorbing centers or which, in any case, would require very thick samples to be detected in absorption.

The basic experimental apparatus has been described elsewhere.[12] In the present case, however, the spectra were corrected for the system response. The excitation spectra were usually recorded by monitoring the strong R-line luminescence, but in order to observe the corresponding transition in absorption (i.e., the $^4A_{2g} \rightarrow {}^2E_g$ zero-phonon transition) we also observed the excitation spectrum of the $^2E_g(n=0) \rightarrow {}^4A_{2g}(n=1)$ sideband at about 11 250 cm^{-1}.

In Fig. 1 the low-resolution ($\sim$10-Å) excitation spectrum of the R line is reported. The broad and intense bands centered at $\sim$14 000 and 19 000 cm^{-1} correspond to the $^4A_{2g} \rightarrow {}^4T_{2g}$ and $^4A_{2g} \rightarrow {}^4T_{1g}$ transitions, respectively.[3] In Fig. 2 we report the low-energy side of the spectrum, taken with higher resolution (~ 5 cm^{-1}). This figure shows, in order of increasing energy, the sideband of the R line, the two zero-phonon lines $^4A_{2g} \rightarrow {}^2T_{1g}$ (Γ_8) and $^4A_{2g} \rightarrow {}^2T_{1g}$ (Γ_6) split by spin-orbit interaction, the sidebands of these lines, and the much more intense structure of the zero-phonon $^4A_{2g} \rightarrow {}^4T_{2g}$ transition. The spectra were recorded at 8 K to prevent "hot bands" due to transitions of the type $^4A_{2g}(n \neq 0) \rightarrow {}^4T_{2g}(n=0)$ which, because of the much larger absorption probability of the $^4T_{2g}$ state, even at 77 K are comparable in intensity to the $^2T_{1g}$ sidebands and partially mask them. Spectra at higher resolution (~ 1.5 cm^{-1}) were taken to investigate the shape of the $^2T_{1g}$ and $^4T_{2g}$ zero-phonon lines (Figs. 3 and 4). Figure 5 shows the excitation spectrum (5-cm^{-1} resolution) of the

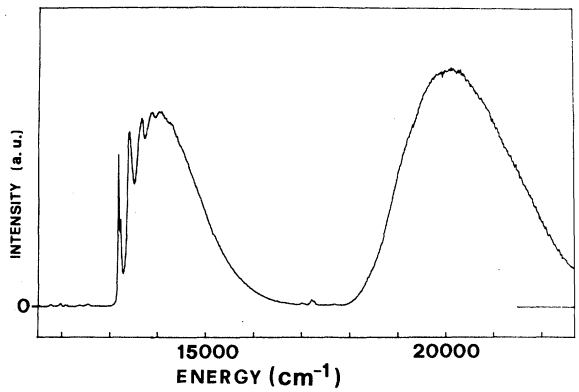

FIG. 1. Excitation spectrum of MgO:V^{2+} at 8 K. The two main bands correspond to $^4A_{2g} \rightarrow {}^4T_{2g}$ and $^4A_{2g} \rightarrow {}^4T_{1g}$ transitions. The weaker features are evidenced in the following figures. Slit width 10 Å.

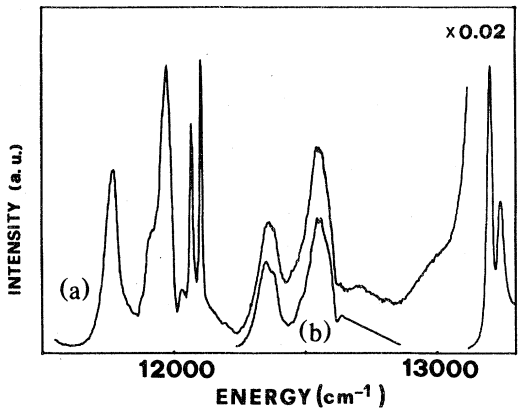

FIG. 2. (a) Low-energy side of the experimental excitation spectrum of MgO:V^{2+} at 8 K, including for comparison the zero-phonon line of $^4T_{2g}$. Slit width 5 cm^{-1}. (b) Computed sideband relative to the $^2T_{1g}$ state.

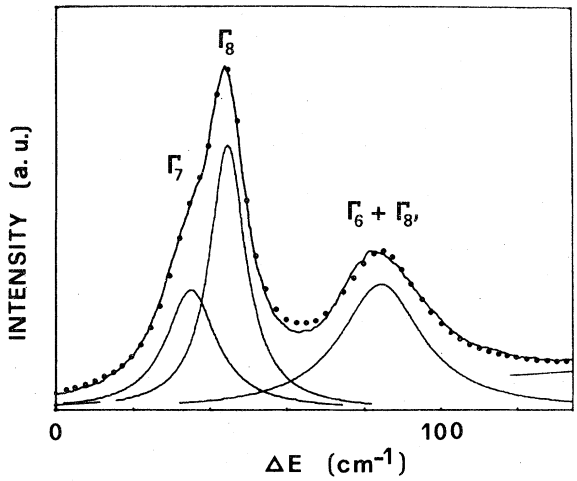

FIG. 4. Shape of the $^4T_{2g}$ zero-phonon line at 8 K, resolution 1.5 cm^{-1}. Full line: experimental; dots: fit as a sum of underlying Lorentzians. The tail of the phonon sideband has been subtracted. Labels indicate the relative vibronic states.

spectral zone between the broad $^4T_{2g}$ and $^4T_{1g}$ bands, where the absorption due to $^2T_{2g}$ is observed.

The width ($\sim$100 cm^{-1}) of the more intense features indicates these to be sidebands. As for the zero-phonon lines corresponding to transitions to the Γ_8 and Γ_7 split components of $^2T_{2g}$, only a very weak structure at $\sim$16 750 cm^{-1} can be observed which is superimposed on the tail of $^4T_{2g}$. More accurate measurements clearly evidenced the Fano-antiresonance shape[13–15] of such structure, but could not unravel the other component of the doublet. A somewhat arbitrary subtraction of the background due to $^4T_{2g}$ and $^4T_{1g}$ bands may serve to better visualize the shape of $^2T_{2g}$ absorption, as shown in Fig. 5(b).

The main results of the present measurements are summarized in Tables I and II. All intensities in Table I are normalized to the R-line intensity whose excitation spectrum, as mentioned, was recorded by detecting its 11 250-cm^{-1} sideband emission: such excitation spectrum, as expected, is in all respects similar to the ones of Figs. 1–5, because once the system has relaxed into the ^2E_g ground vibronic level, the various deexcitation mechanisms are in any case the same.

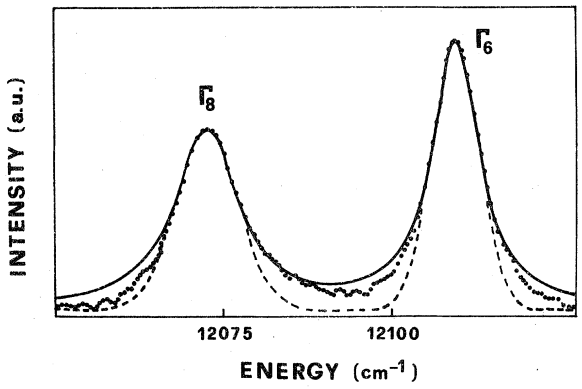

FIG. 3. Shape of the $^2T_{1g}$ zero-phonon line at 8 K. Dots: experimental (resolution 1.5 cm^{-1}); full line: Lorentzian fit; dashed line: Gaussian fit. The widths are 8 and 6 cm^{-1} for Γ_8 and Γ_6, respectively.

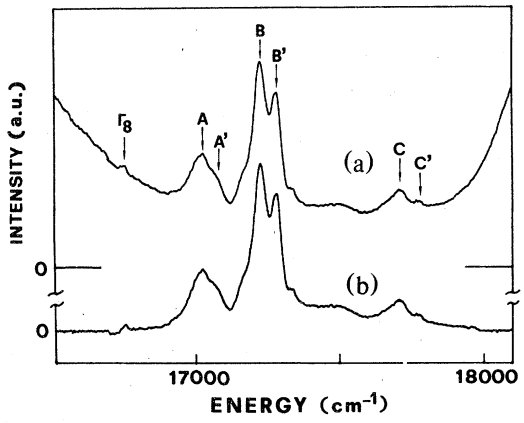

FIG. 5. (a) Excitation spectrum of the $^4A_{2g} \rightarrow {}^2T_{2g}$ transition at 77 K, 5-cm^{-1} resolution. (b) After subtraction of the $^4T_{1g}$ and $^4T_{2g}$ tails. The weak antiresonance feature at low energy is tentatively assigned to the Γ_8 zero-phonon transition.

TABLE I. Experimental and calculated (static-crystal-field) energies and intensities for transitions from the $^4A_{2g}$ ground state. Parameter values (cm^{-1}): 10 Dq = 14 000; $C = 2330$; $B = 620$; $\zeta = 136$. Experimental energies and intensities of $\langle E_{MD} \rangle$ and $\langle E_{ED} \rangle$ are evaluated as explained in the text. ZPL: zero-phonon line; SB: sideband.

State		Energy Expt.	Energy Calc.	Intensity Expt.	Intensity Calc.
^2E_g	ZPL	11 502	11 479	1	1
	SB	11 770	...	4.5	...
	SB	11 980	...		...
$^2T_{1g}$	ZPL (Γ_8)	12 073	12 056	0.26	0.33
	ZPL (Γ_6)	12 106	12 098	0.28	0.32
	SB	12 360	...	5.0	...
	SB	12 550	...		...
$^4T_{2g}$ (SB)	$\langle E \rangle$	14 330	...	2500	...
	$\langle E_{MD} \rangle$	14 000	14 000	400	600
	$\langle E_{ED} \rangle$	14 400	...	2100	...
$^2T_{2g}$	ZPL (Γ_8)	16 750	17 292	0.05	0.18
	ZPL (Γ_7)	16 800	17 366	...	0.01
	SB	17 020	...	12	...
	SB	17 070	...		...
	SB	17 220	...		...
	SB	17 280	...		...
$^4T_{1g}$ (SB)	$\langle E \rangle$	20 400	...	5000	...
	$\langle E_{MD} \rangle$	20 000	...	...	...
	$\langle E_{ED} \rangle$	20 400	...	5000	...

III. MAGNETIC DIPOLE TRANSITIONS

The Hamiltonian of the system is

$$H = H_{el} + H_{so} + H_{vib} + H_{el-vib} = H_{el} + \sum_i \vec{\Gamma}_i \cdot \vec{s}_i + \frac{1}{2} \sum_j \left(\frac{P^2}{M} + K_j Q_j^2 \right) + \sum_j \frac{\partial V}{\partial Q_j} Q_j \ , \quad (1)$$

where H_{el} contains the kinetic energy of the electrons, the Coulomb, exchange, and static crystal-field interactions; H_{so} is the spin-orbit interaction; H_{vib} is the energy of the nuclei in the harmonic approximation; H_{el-vib} contains the electron-vibration interaction terms which are linear in the even and odd normal coordinates. Since V^{2+} is at a site of cubic symmetry, the vibronic eigenstates of Eq. (1) have definite parity; odd vibrations however will mix electronic states of opposite parity. As said, for V^{2+} the lowest states derive from the d^3 electronic configuration and are all even; the odd electronic states lie much higher in energy and their positions, symmetries, and relative electronic configurations are not known: consequently, we will neglect the odd coordinates in Eq. (1), and will consider them later in a perturbative way. But even if one limits oneself to the d^3 configuration, it is practically impossible to diagonalize Hamiltonian (1) even including only a few vibrational states. Therefore, $H_{el} + H_{so}$ is first diagonalized within the d^3 configuration, and subsequently $H_{vib} + H_{el-vib} + H'_{so}$ is diagonalized within the levels of interest, being H'_{so} a phenomenological spin-orbit Hamiltonian[16]

$$H'_{so} = \lambda \vec{L} \cdot \vec{S} + \mu (\vec{L} \cdot \vec{S})^2 + \rho (L_x^2 S_x^2 + L_y^2 S_y^2 + L_z^2 S_z^2) \ . \quad (2)$$

TABLE II. Relative energies (cm^{-1}) and intensities of the components of the $^4A_{2g} \rightarrow {}^4T_{2g}$ zero-phonon line. Intensities are normalized to $I(\Gamma_7)$.

State	Energy Expt.	Energy Calc.	Intensity Expt.	Intensity Calc.
Γ_7	0	0	1	1
Γ_8	10	20.3	1.6	1.7
Γ_6	49	54.4	1.7	0.61
$\Gamma_{8'}$	49	57.1		1.18

The matrix elements of the $H_{el}+H_{so}$ for the d^3 configuration have been calculated by Eisenstein[17] in the strong-field basis. The calculation involves at least four parameters: the crystal-field splitting, 10 Dq; the Racah parameters B and C; and the spin-orbit coupling constant ζ. In these regards, it should be noted that the experimental energies to be fitted are those corresponding to the centroid of the MD portion of the band; in fact, it is known that the electron-phonon interaction lowers the ZPL but leaves the centroid unaffected. It is not trivial to subtract from the experimental spectra the ED contribution. For the ^2E_g, $^2T_{1g}$, and $^2T_{2g}$ states (deriving from the t_2^3 electronic configuration) we will assume the MD intensity to be almost completely concentrated in the ZPL's. This is equivalent to assuming that the relative sidebands are completely ED; this seems to be the case for ^2E_g,[5,7] but the $^2T_{1g}$ and $^2T_{2g}$ states could possibly be a little more coupled to even vibrations. For $^4T_{1g}$, it is known that the intensity is mostly ED; on the other hand, the width of the band must be due to even phonons, because odd multiphonon interactions are not conceivable due to their weak coupling; thus, the band is thought of as originating from transitions involving creation of one odd phonon and many even phonons. If then we assume that the density of odd-phonon states is not very much different to that relative to the ^2E_g state, we can find the energy of the centroid of the MD part of the band by subtracting the average energy of one odd phonon ($\sim$400 cm^{-1}) from the centroid of the observed band.

A similar argument applies to $^4T_{2g}$, but by considering that in this case the intensity is due to both MD and ED, the first moment resulting from the two contributions is

$$\langle E\rangle = \frac{I_{MD}\langle E_{MD}\rangle + I_{Ed}\langle E_{ED}\rangle}{I_{ED}+I_{MD}} \quad . \tag{3}$$

The intensity ratio I_{ED}/I_{MD} of the ED to the MD contributions which appears in Eq. (3), is probably the same as in the case of the $^2E_g \rightarrow {}^4A_{2g}$ emission.[7] In the latter transition a ratio 5.6 between the sideband and the ZPL intensities is observed.[5] It should be noted however that even a weak MD contribution to the intensity of the sideband would lower very much the above ratio. From the preceding discussion and from Eq. (3) we can estimate $\langle E_{MD}\rangle = 14\,000$ cm^{-1}. The values of all the estimated energies (apart from $^4T_{2g}$ ZPL which will be discussed in Sec. V) are summarized in Table I first column.

The results of the diagonalization of Hamiltonian $H_{el}+H_{so}$ are reported in the second column; as regards the choice of the parameters, 10Dq is the energy difference $E(^4T_{2g})-E(^4A_{2g}) = 14\,000$ cm^{-1}; for B and C, we have kept the ratio $C/B = 3.7$, which is the free ion value[18] and we have found the best fit for $B = 620$ cm^{-1} and $C = 2330$ cm^{-1}: these values are reduced by a factor $k = 0.81$ with respect to the free ion values, which is reasonable in view of the covalency quenching. The choice of the spin-orbit parameter ζ is not trivial; in fact, the only observed first-order spin-orbit splitting concerns the ZPL of $^4T_{2g}$ which, however, is quenched by the Ham effect[19–21] by an amount which is not known at this stage. On the other hand, the splittings of the $^2T_{1g}$ and $^2T_{2g}$ states derive from higher-order coupling to many states, some of which suffer strong electron-phonon interaction, which is not taken into account in the diagonalization of the crystal-field Hamiltonian; therefore, even though such splittings are strongly dependent on ζ, it is not easy to deduce from a best-fit procedure a precise value of ζ because many other parameters are important to determine the splittings. Then, to keep the number of parameters as limited as possible, we used for ζ the free-ion value (167 cm^{-1}), reduced by the same factor 0.81 as B and C; i.e., $\zeta = 136$ cm^{-1}. These values of ζ and k are consistent with the observed g values of $^4A_{2g}$ ($g = 1.980\,3 \pm 0.000\,5$)[1] and of ^2E_g ($g = 1.88 \pm 0.04$)[3]; in fact using Eqs. (21) and (27) of Ref. 10 we get $g(^4A_{2g}) = 1.980\,8$ and $g(^2E_g) = 1.90$. Moreover, the experimental energies are satisfactorily reproduced except for $^2T_{2g}$, as usual in d^3 systems.[8,22]

As regards the MD intensities, the magnetic dipole operator is

$$\vec{M} = -\sum_i (k\,\vec{l}_i + 2\vec{s}_i) \quad ,$$

where $0 < k < 1$ is the quenching factor of the orbital angular momentum due to covalency and the summation is over the valence electrons. $\vec{M}$ transforms according to the $T_{1g}(\Gamma_4^+)$ irreducible representation of O_h and it connects states with the same spin multiplicity; more specifically the only allowed MD transition from the ground $^4A_{2g}$ state is to $^4T_{2g}$, while all of the doublet states ($^2T_{1g}$, $^2T_{2g}$, ^2E_g) are connected to each other by $\vec{M}$.

The matrix elements of M_z among the strong-crystal-field states of the d^3 configuration have been computed by Eisenstein,[17] and in absence of any external perturbation, they are sufficient to evaluate all of the transition probabilities among d^3 states. As regards the quenching factor k, its knowledge is only required to compute absolute transition probabilities: in fact, the spin part of $\vec{M}$ is rather unimportant for the transition of interest to us, so that all of the transition probabilities are proportional to k^2. This derives from the fact that the $^4A_{2g} \rightarrow {}^4T_{2g}$ transition involves only the orbital part of $\vec{M}$ [see discussion following Eq. (4)].

The MD computed intensities are reported in the last column of Table I, and are normalized to the intensity of the ^2E_g ZPL. Even though the wave functions are in general very sensitive to small variations of the parameters values, thus making agreement

between experiment and theory problematic, our computed values compare very favorably with experiment; the relatively bad agreement in the case of $^2T_{2g}$ is due to the high background intensity of the $^4T_{2g}$ tail with which $^2T_{2g}$ antiresonates (see Fig. 5); moreover in the $^4A_{2g} \rightarrow {}^2T_{2g}$ transition contributions from many d^3 states are important and mutually interfering, thus rendering the theoretical estimate less reliable. In fact, the states are not pure crystals-field states, but are mixed by spin-orbit and Coulomb interactions. For instance we have for the ground state:

$$|^4A_{2g}^*, \Gamma_8, \gamma\rangle = a\,|^4A_{2g}, \Gamma_8, \gamma\rangle + \sum_i b_i |\Gamma_8^i, \gamma\rangle \quad , \qquad (4)$$

where γ is a substate of the Γ_8 quartet, and Γ_8^i refers to the remaining 20 states of the d^3 configuration. Our diagonalization yields $a^2 = 0.999\,7$, and since only $^4A_{2g} \rightarrow {}^4T_{2g}$ transitions are MD allowed, for any excited state which contains an appreciable amount of $^4T_{2g}$ the only important term of Eq. (4) is the first. This is valid for all the excited states we are considering except $^2T_{2g}$,[23] so that in this case all of the terms on the right side of Eq. (4) must be taken into account.

IV. ELECTRIC DIPOLE TRANSITIONS

In this section we will consider only ED transitions relative to the ^2E_g, $^2T_{1g}$, $^2T_{2g}$ states which are weakly coupled to vibrations: for these states, in fact, the shape of the ED sidebands is easily observed and contrary to $^4T_{2g}$ and $^4T_{1g}$ states there are no MD vibronic transitions which complicate the spectra. It is therefore easy, for the weakly coupled states, to compare intensities and shapes of the ED sidebands, which reproduce the one-odd-phonon density of states.

As it results from Figs. 2 and 5 and from Table I, the results of interest here are the following.

(1) The absorption sideband of ^2E_g does not appreciably differ from the emission one, both in shape and in intensity relative to the ZPL, at least up to 570 cm^{-1} from the ZPL, where it is not superimposed to the $^2T_{1g}$ state.

(2) The sideband-to-ZPL intensity ratio, R, is not the same for ^2E_g, $^2T_{1g}$, and $^2T_{2g}$. More specifically, $R(^2T_{1g}) \simeq 1.5R(^2E_g)$ and $R(^2T_{2g}) \simeq 50R(^2E_g)$; also, the ratio of the acoustical-to optical-phonon-contribution changes: this is smaller for $^2T_{2g}$ than it is for ^2E_g and $^2T_{1g}$.

Item 1 implies, that, as expected, the projected density of vibrational states is very similar when the impurity ion is in the $^4A_{2g}$ or ^2E_g states. In these regards, it may be interesting to note that a similar behavior is observed in MgO:Cr^{3+},[9] whereas the situation is quite different in ruby.[24]

Item 2 needs a deeper discussion especially in connection with previous assumptions[2,7] on the mechanisms of ED transitions. The Hamiltonian coupling states of different parity in cubic symmetry has the form[7]

$$H_u = \sum_{\Gamma_\gamma} \frac{\partial V}{\partial Q_{\Gamma_\gamma}} Q_{\Gamma_\gamma} \quad , \qquad (5)$$

where V is the electron-ion potential, and Q_{Γ_γ} is the normal coordinate transforming as the γ component of the odd irreducible representation Γ. However since the ground state is a spin quartet, transitions to the doublet states are allowed only through spin-orbit mixing. From our diagonalization it results that the $^4A_{2g}$ state is not spin mixed to any significant extent. Therefore, two basic mechanisms are conceivable which can give oscillator strength to the ED sidebands, according to whether the spin-orbit interaction is considered to be active among even or odd states, respectively:

$$\text{(a)}\quad {}^4A_{2g} \overset{P}{\rightarrow} {}^4\Gamma_u;\ {}^4\Gamma_u \overset{H_u}{\rightarrow} {}^4\Gamma_g;\ {}^4\Gamma_g \overset{H_{so}}{\rightarrow} {}^2\Gamma_g$$

or, alternatively:

$$\text{(b)}\quad {}^4A_{2g} \overset{H_u}{\rightarrow} {}^4\Gamma_u;\ {}^4\Gamma_u \overset{P}{\rightarrow} {}^4\Gamma_g;\ {}^4\Gamma_g \overset{H_{so}}{\rightarrow} {}^2\Gamma_g$$

$$\text{(b)}\quad {}^4A_{2g} \overset{P}{\rightarrow} {}^4\Gamma_u;\ {}^4\Gamma_u \overset{H_{so}}{\rightarrow} {}^2\Gamma_u;\ {}^2\Gamma_u \overset{H_u}{\rightarrow} {}^2\Gamma_g$$

or, alternatively:

$$\text{(b)}\quad {}^4A_{2g} \overset{H_u}{\rightarrow} {}^4\Gamma_u;\ {}^4\Gamma_u \overset{H_{so}}{\rightarrow} {}^2\Gamma_u;\ {}^2\Gamma_u \overset{P}{\rightarrow} {}^2\Gamma_g \quad ,$$

where P is the electric dipole operator, $^{2s+1}\Gamma_u$ are the intermediate odd-parity states.

Manson and Shah[7] interpreted their MCP data by assuming only mechanism (a) to be active and by neglecting the contribution of the $^4T_{1g}$ state to it. If this were true, the R's relative to different doublet states should be the same. In fact, if only $^4T_{2g} - {}^2\Gamma_g$ spin-orbit coupling is important, from the formula at the bottom of page 1996 of Ref. 7 it appears that only the T_{1g} component of the operator $H_u \otimes P$ induces the transitions, irrespective of the symmetry of the odd phonon involved. Therefore, the operator which induces the transitions has the same symmetry as the MD operator. As a consequence, the intensity of a vibronic transition $^4A_{2g} \rightarrow {}^2\Gamma_g (n_{\Gamma_u} = 1)$ is proportional to the intensity of the relative ZPL, for all $^2\Gamma_g$, so that we can, for instance, obtain the sideband of $^2T_{1g}$ (which is split by spin-orbit interaction) by a superposition of two ^2E_g-like sidebands originating from the two split zero-phonon peaks, and normalized to the relative intensities of these peaks with respect to ^2E_g ZPL. This procedure has been used to obtain Fig. 2(b): it is clear from this figure that the shape of the $^2T_{1g}$ sideband is quite well reproduced in this

way. Moreover, the fact that $R(^2T_{1g}) \sim 1.5R(^2E_g)$ (which is not a big difference), implies that for ^2E_g and $^2T_{1g}$ mechanism (a) must actually be the most important. The situation is quite different for $^2T_{2g}$, where $R(^2T_{2g}) \sim 50R(^2E_g)$: this indicates that for this state mechanism (b) must play an important role; another source of difference with respect to ^2E_g and $^2T_{1g}$ is probably the spin-orbit coupling to $^4T_{1g}$, which is itself strongly coupled to odd vibrations. Actually, our diagonalization of Hamiltonian (1) indicates that $^2T_{2g}$ is more admixed with $^4T_{1g}$ than it is with $^4T_{2g}$. It is then reasonable to think that, within mechanism (a), coupling to $^4T_{2g}$ is negligible with respect to coupling to $^4T_{1g}$. More quantitatively, the ratio of the $^2T_{2g}$ to $^4T_{1g}$ sidebands is of the same order of magnitude as the square of the $^4T_{1g} - {}^2T_{2g}$ spin-orbit mixing coefficient.

It should also be noted that while the $^4T_{1g} - {}^2E_g$ mixing coefficient is practically zero,[18] a small $^4T_{1g}$ contribution is present in $^2T_{1g}$, in qualitative agreement with $R(^2T_{1g}) > R(^2E_g)$.

Going back to $^2T_{2g}$, the fact that its sideband is mainly due to spin-orbit coupling to $^4T_{1g}$ explains the quite different shape of this sideband with respect to $^2T_{1g}$ and ^2E_g ones, because it should reflect the projected density of states when the impurity is in the $^4T_{1g}$ state. The prominent features of the sideband are peaks B and B' of Fig. 5, which are thought of as originating from two spin-orbit split ZPL's, only one of which is observed (probably Γ_8); the spin-orbit splitting is also observed in the acoustical (A,A') band and in the $C\,C'$ features. The energy of the B, B' features $[E(B) - E(\Gamma_8) \simeq 500\ \text{cm}^{-1}]$ is practically coincident with that observed by Manson and Shah[7] in the emission sideband of ^2E_g, and attributed by these authors to T_{2u} vibrations. This seems to indicate that, contrary to $^4T_{2g}$, $^4T_{1g}$ is more or less equally coupled to T_{2u} and T_{1u} modes.

V. SHAPE OF THE ZERO-PHONON LINES

In MgO:V^{2+} ZP transitions to four electronic excited states are observed: ^2E_g, $^2T_{1g}$, $^4T_{2g}$, and $^2T_{2g}$; among these, only ^2E is observed in emission at low temperature. The ^2E_g ZPL is not structured because the spin-orbit interaction is not active, while the remaining three ZPL's should be doublets ($^2T_{1g}$, $^2T_{2g}$) or a quartet ($^4T_{2g}$). Moreover, contrary to the spin-doublet states, the $^4T_{2g}$ state is quite strongly coupled to lattice vibrations, giving rise to a broad and intense phonon sideband, in addition to the ZPL (see Table I). The ^2E_g-ZPL has been widely studied in the literature[3,25]; at low temperature it has a nearly Gaussian shape whose width is sample dependent (0.4 cm^{-1} in our sample), as is typical of strain-induced inhomogeneous broadening.

The $^4T_{2g}$-ZPL has also been the object of many experimental and theoretical studies. Sturge[4] first observed only two broad components split of about 40 cm^{-1}, the lower-energy one being about two times as intense as the high-energy one. Many things have been said about this shape: (i) the spin-orbit interaction of $^4T_{2g}$ is completely quenched by the Jahn-Teller effect and the observed splitting is an orbital splitting due to some distortions of τ_{2g} type[4,26]; (ii) the spin-orbit interaction is again ineffective, and the observed splitting actually derives from transitions to different vibrational levels, in that some excited τ_{2g} vibrational levels of $^4T_{2g}$ are lowered in energy and mixed with the ground vibronic level in order to form a pair of nearly degenerate levels, and an excited level, separated by about 40 cm^{-1},[27-29] and (iii) the splitting is due to spin-orbit interaction, but some mechanism broadens the single lines and does not allow the quartet structure to be observed.[20] Zeeman measurements[21] showed that explanation (iii) is the correct one; recently more accurate Zeeman measurements[30] confirmed such interpretation and further showed that the observed lines are actually three (see also our measurements in Fig. 4). Manson and Sturge[30] also found that the spectrum at 2 K is in practice completely (~98%) circularly polarized: the low-energy doublet right, the high-energy component left. This allows assignment of the peaks to the spin-orbit sublevels relative to $^4T_{2g}$ as shown in Fig. 4. In this figure a deconvolution of the spectrum with three Lorentzian curves is also shown. We tried to fit the spectrum with Gaussian curves as well, but with much poorer results.

From Figs. 1 and 2 we can see that the ZPL is not well separated from the phonon sideband; thus, in order to be able to measure the intensities of the various components of the ZPL we had to subtract (somewhat arbitrarily) the underlying contribution of the sideband. The splittings, intensities and widths of the ZPL components are reported in Table II.

The observed splittings can be qualitatively reproduced introducing a Jahn-Teller coupling to ϵ_g modes whose effect is a spin-orbit quenching.[19] However, the quenched first-order spin-orbit interaction alone cannot account for the relative magnitude of the observed splittings. In fact, the predicted ratio $(E_{8',6} - E_8)/(E_8 - E_7)$ is 1.67, whereas the experimental value is ~4. Also, we have to explain the origin of the widths of the ZPL's and of their relative intensities. The first characteristic will be considered later; as regards the relative intensities it has been recently shown[31,32] that it is a general consequence of the dynamical Jahn-Teller effect to reduce the intensity of the higher-energy spin-orbit components with respect to static-crystal-field calculations.

Let us now consider the problem more quantitatively, within the cluster model approximation. The

Hamiltonian of the system in $^4T_{2g}$ state is

$$H = H'_{so} + H_{vib} + H_{JT} \ , \tag{6}$$

where H'_{so} is given by Eq. (2), and H_{JT} can be expressed as[19]

$$H_{JT} = b(Q_\epsilon E_\epsilon + Q_\theta E_\theta) \ , \tag{7}$$

where E_ϵ and E_θ are the matrices as given by Ham[19] and b is the coupling constant for ϵ_g modes. Neglecting trigonal modes of τ_{2g} type in Eq. (7) is justified because the relative coupling constant is about one order of magnitude smaller than b.[33] As regards the spin-orbit parameters λ, μ, and ρ they can be deduced by comparing the diagonalization of the crystal-field Hamiltonian to the solution of the spin-orbit Hamiltonian.[34] The values of λ, μ, and ρ suitable for MgO:V^{2+} result to be[35] $\lambda = 30.27$ cm^{-1}, $\mu = 0.37$ cm^{-1}, and $\rho = 3.5$ cm^{-1}. Hamiltonian (6) has been diagonalized including six ϵ_g vibrational states, for various values of b and of $\hbar\omega_\epsilon$; in Fig. 6 the ground-state levels are reported, as a function of $E_{JT} = 2b^2/3K_\epsilon$, for $\hbar\omega_\epsilon = 200$ cm^{-1}. E_{JT} is the energy lowering of the minimum in the absence of spin-orbit interaction. In Fig. 6, the triangles are the experimental energies; the best fit is obtained for $E_{JT}/\hbar\omega_\epsilon \simeq 0.5$, and is almost independent of the value of $\hbar\omega_\epsilon$, in qualitative agreement with the approximate first-order theory of Ham which gives for the effective coupling constant

$$\lambda_{eff} = \lambda \exp(-\tfrac{3}{2} E_{JT}/\hbar\omega_\epsilon) \ .$$

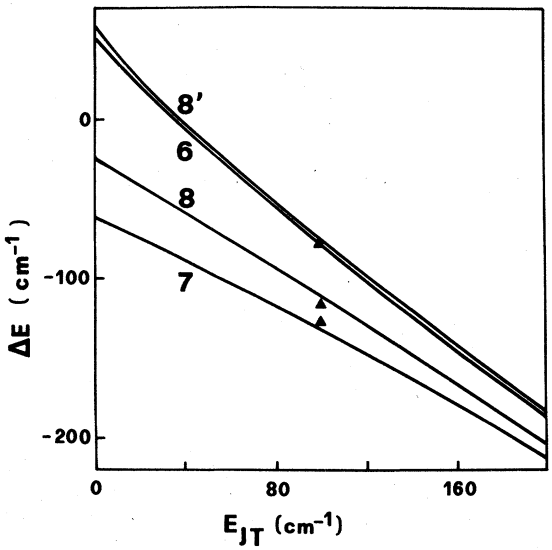

FIG. 6. Energy levels of $^4T_{2g}$ zero-phonon states: full lines, computed by diagonalizing Hamiltonian (6). Triangles represent experimental splittings. Energy zero corresponds to the energy of $^4T_{2g}$ without Jahn-Teller effect and spin-orbit interaction. E_{JT} is defined in the text. The labels 7, 8, 6, and 8′ refer to the irreducible representations Γ_i of O_h^*.

At the present stage of the theory, if one wishes to fit the overall splitting, one obtains too high a value for the $E_7 - E_8$ splitting, whereas the coalescence of E_6 and $E_{8'}$ is well accounted for.

Contrary to the energy splittings, which depend almost exclusively on $E_{JT}/\hbar\omega_\epsilon$ (there is little high-order dependence on $\hbar\omega_\epsilon$), the intensities of the various transitions are strongly dependent on the phonon energy[32]; we have used the method of Ref. 32 to deduce an effective value of $\hbar\omega_\epsilon$ which gives a good fitting of the observed intensity ratios. The method gives $\hbar\omega_\epsilon = 200$ cm^{-1}. In Fig. 7(a) the relative, degeneracy-normalized intensities are reported as a function of E_{JT}. The bar indicating the experimental intensity-ratio is reported at $E_{JT}/\hbar\omega_\epsilon = 0.5$; such value has been deduced by fitting the splitting. We note that even quite a small Jahn-Teller effect can produce observable reductions of the relative intensities. In Fig. 7(b) the mixing between Γ_8 and $\Gamma_{8'}$ states is shown. Both second-order spin-orbit interaction and Jahn-Teller effect mix these states, but the two effects tend to cancel each other. This is due to the positive sign of $\mu + \rho$ ($\mu + \rho \sim 4$ cm^{-1}) in Hamiltonian (2) contrary to what happens in $KMgF_3$:V^{2+} ($\mu + \rho \sim -6.5$ cm^{-1}).[36] Our diagonalization [see Fig. 7(b)] gives $\sim 10^{-3}$ for the square of the mixing coef-

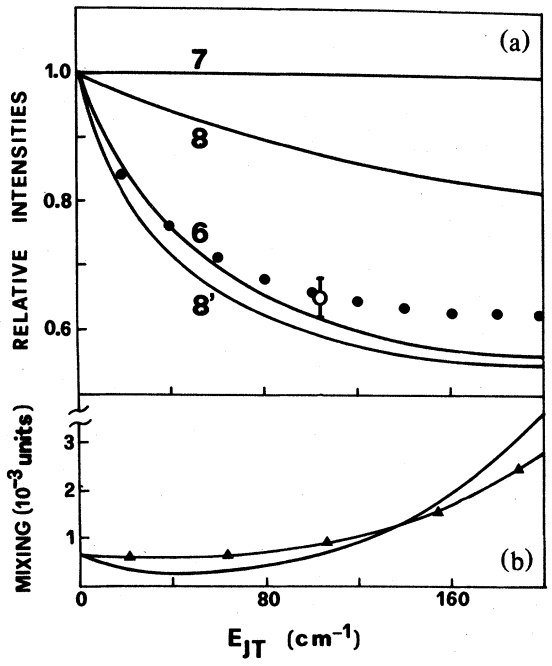

FIG. 7. (a) Degeneracy-normalized relative intensities of the spin-orbit sublevels of the $^4T_{2g}$ zero-phonon line. Dots: $[I(6) + 2I(8')]/[I(7) + 2I(8)]$; labels same as for Fig. 6. The bar indicates experimental ratio, and should be compared to the dots. (b) Squared mixing coefficients between Γ_8 and $\Gamma_{8'}$ states; full line: Γ_8 in $\Gamma_{8'}$; triangles: $\Gamma_{8'}$ in Γ_8.

ficients between Γ_8 and $\Gamma_{8'}$ for $E_{JT}/\hbar\omega_\epsilon = 0.5$. These coefficients just give the relative intensity of the inversely circularly polarized absorption with respect to the directly polarized one in Zeeman experiments at low temperature (neglecting the magnetic field mixing). The recent measurements of Manson and Sturge[30] (mixing less than 2%) are in full agreement with our calculation.

The phonon energy used to fit the intensities has definite physical meaning only within the framework of the cluster model. For MgO:V^{2+} such model involving only one definite vibrational energy $\hbar\omega_\epsilon$ seems to be an oversimplification: in fact, the phonon sideband's low-energy tail is more or less superimposed on the ZPL, so that the value of 200 cm^{-1} we find is to be understood as the effective phonon energy one has to use if one wishes to employ the cluster model. This value may not correspond to any of the peaks of the density of states of the crystal, nor even to its average energy; in fact the procedure of Ref. 32 tends to give a value of $\hbar\omega_\epsilon$ which is smaller than the average energy, because the intensity-quenching effect is larger for low-energy phonons.

Phonon structures are clearly observable in the sideband, which were early interpreted by Sturge as an uniquantal progression of modes due to a rather strong JTE.[26] From the previous discussion, however, we have seen E_{JT} to be of the order of 100 cm^{-1}, while the total lowering of the minimum is about 800 cm^{-1}; this implies that the A_{1g} modes must be the most coupled. This is consistent with theoretical estimates[33] of the lowering energies E, which give $\Delta E(A_{1g})/\Delta E(\epsilon_g) \sim 2$ and $\Delta E(A_{1g})/\Delta E(\tau_{2g}) \sim 25$. One is then led to think that if the structures are due to even phonons, these are probably of A_{1g} symmetry; on the other hand, most of the band should be of electric dipole character induced by odd phonons whose density of states has two peaks (acoustical and optical branches) at 270 and 490 cm^{-1}, which correspond well to the first two structures of the absorption band. Recent stress measurements[9] seem to indicate however that the structures are due to even phonons. Further experimental investigation is necessary to establish firmly the symmetry of these phonons.

As regards the width of the components of the ZPL, it can be shown,[37] in the case of $^4T_{2g}$, that it derives from fast ($\sim 10^{-13}$ sec) nonradiative transitions to $^2T_{1g}$ and ^2E_g as in ruby[38]: in other words, the width of the ZPL is the natural linewidth due to the uncertainty principle. This is due to the interlevel spin-orbit interaction which mixes zero-phonon states of $^4T_{2g}$ to many-phonon states of $^2T_{1g}$ and ^2E_g, causing broadening and Lamb shift of the ZPL.[37,39,40] In this way the observed splittings can also be better reproduced. Random-strain-induced inhomogeneous broadening seems to give a negligible contribution in this case, which is consistent with the Lorentzian shape of the lines.

A similar calculation on the $^2T_{1g}$ ZPL has not been possible as yet because the effective phonon-spectrum, which governs the $^2T_{1g} \rightarrow {}^2E_g$ nonradiative transitions, is not known. As can be seen from Fig. 3, the shape is more or less Lorentzian in this case also, even though a contribution from inhomogeneous broadening, which yields a Gaussian shape[38] to the $^2E_g \rightarrow {}^4A_{2g}$ emission, cannot be ruled out. It should be noted however that in our sample the $^2E_g \rightarrow {}^4A_{2g}$ emission is only 0.4 cm^{-1} broad, whereas $^2T_{1g}$'s widths are of the order of 5–10 cm^{-1}.

ACKNOWLEDGMENT

Work partially supported by CNR, Contract No. 79-02110-02.

[1]W. Low, Phys. Rev. 40, 55 (1958).
[2]S. Sugano, A. L. Schawlow, and F. Varsanyi, Phys. Rev. 120, 2045 (1960).
[3]M. D. Sturge, Phys. Rev. 130, 639 (1963); 131, 1456 (1963).
[4]M. D. Sturge, Phys. Rev. 140, A880 (1965).
[5]B. Di Bartolo and R. Peccei, Phys. Rev. 137, A1770 (1965); B. Di Bartolo and R. C. Powell, Nuovo Cimento B 66, 21 (1970).
[6]S. E. Stokowski, S. A. Johnson, and P. L. Scott, Phys. Rev. 147, 544 (1966).
[7]N. B. Manson and G. A. Shah, J. Phys. C 10, 1991 (1977).
[8]W. M. Fairbank, Jr., and G. K. Klauminzer, Phys. Rev. B 7, 500 (1973).
[9]A. Boyrivent, E. Duval, M. Montagna, G. Viliani, and O. Pilla, J. Phys. C 12, L803 (1979).
[10]R. M. Macfarlane, Phys. Rev. B 1, 989 (1970).
[11]J. P. Larkin, G. F. Imbusch, and F. Dravnieks, Phys. Rev. B 7, 495 (1973).
[12]O. Pilla, M. Montagna, G. Viliani, and S. Santucci, Phys. Rev. B 21, 4859 (1980).
[13]U. Fano, Phys. Rev. 124, 1866 (1961).
[14]M. D. Sturge, J. Chem. Phys. 51, 1254 (1969).
[15]M. D. Sturge, H. J. Guggenheim, and M. H. L. Pryce, Phys. Rev. B 2, 2459 (1970).
[16]J. Kanamori, Prog. Theor. Phys. 17, 177 (1957).
[17]J. C. Eisenstein, J. Chem. Phys. 34, 1628 (1961).
[18]J. S. Griffith, *The Theory of Transition-Metal Ions* (Cambridge University Press, Cambridge, 1961).
[19]F. S. Ham, Phys. Rev. 138, A1727 (1965).
[20]A. Ranfagni and G. Viliani, Phys. Status Solidi B 84, 393 (1977).

[21]G. Viliani, M. Montagna, O. Pilla, A. Fontana, M. Bacci, and A. Ranfagni, J. Phys. C 11, L439 (1978).
[22]S. Sugano and M. Peter, Phys. Rev. 122, 381 (1961).
[23]The $^2T_{2g}$ state is itself mixed in the $^4A_{2g}$ ground state.
[24]D. F. Nelson and M. D. Sturge, Phys. Rev. 137, A1117 (1965).
[25]G. F. Imbusch, W. M. Yen, A. L. Schawlow, D. E. McCumber, and M. D. Sturge, Phys. Rev. 133, A1029 (1964).
[26]M. D. Sturge, in *Solid State Physics,* edited by F. Seitz, D. Turnbull, and H. Ehrenreich (Academic, New York, 1967), Vol. 20, p. 91.
[27]F. S. Ham, in *Optical Properties of Ions in Solids,* edited by H. M. Crosswhite and H. W. Moss (Wiley, New York, 1967), p. 357.
[28]M. Bacci, Phys. Lett. 57A, 475 (1976).
[29]M. Bacci, Phys. Status Solidi B 82, 169 (1977).
[30]N. B. Manson and M. D. Sturge (unpublished).
[31]S. Muramatsu and N. Sakamoto, J. Phys. Soc. Jpn. 46, 1273 (1979).
[32]M. Montagna, O. Pilla, and G. Viliani, J. Phys. C 12, L699 (1979).
[33]M. Bacci, Chem. Phys. Lett. 58, 537 (1978); Chem. Phys. 40, 237 (1979); Phys. Status Solidi B 92, 193 (1978); and (private communication).
[34]P. Koidl, Phys. Status Solidi B 74, 477 (1976).
[35]As $^4T_{2g}$ experiences quite a strong electron-phonon interaction which displaces the minimum of its potential surface with respect to the other states, in order to find the correct values of the spin-orbit parameters we cannot use the d^3 diagonalization results as found in the previous sections, which pertain to the $\{Q_i=0\}$ nuclear configuration. It is necessary to diagonalize the d^3-Hamiltonian taking 10 Dq = 12 400 cm^{-1}, which reproduces the $^4T_{2g}-{}^4A_{2g}$ energy difference in emission, instead of 10Dq = 14 000 cm^{-1}, appropriate for absorption. In this way, the effect of the second-order spin-orbit interaction with ^2E_g and $^2T_{1g}$ is increased but still underestimated (see Ref. 40).
[36]M. D. Sturge, Phys. Rev. B 1, 1005 (1970). In $KMgF_3:V^{2+}$ the $^4T_{2g}$ level is lower in energy than ^2E_g and $^2T_{1g}$.
[37]M. Montagna, O. Pilla, and G. Viliani, Phys. Rev. Lett. 45, 1008 (1980).
[38]A. Monteil and E. Duval, J. Lumin. 18–19, 793 (1979).
[39]R. Lacroix *et al.* (unpublished).
[40]B. Di Bartolo, *Optical Interaction of Ions in Solids* (Wiley, New York, 1968).